Research Article

Eco-friendly removal of hexavalent chromium from aqueous solution using natural clay mineral: activation and modification effects

Eman A. Ashour[1] · Maha A. Tony[2]

Abstract

Inexpensive and naturally abundant clay mineral is investigated as a non-toxic and environmentally friendly adsorbent. The clay adsorbent prepared from natural clay (NC) by drying and milling then treated with diluted HCl before calcination to 600 °C. The structural and morphological properties of this modified clay are investigated by Fourier-transform infrared spectroscopy and scanning electron microscope. NC and modified clay at 600 °C (MC600) were applied for hexavalent chromium, Cr(VI), removal from aqueous media via batch adsorption facility. According to the experimental results, the adsorption capacity for chromium removal was calculated (14.3 mg g^{-1}) with a removal efficiency reached to 66% after 90 min of equilibrium time. The sorption matrix indicated that Cr(VI) removal is following the pseudo-second order kinetic model. The experimental data are well fitted with Freundlich isotherm model and the adsorption process is suggested to follow a chemisorption and favourable uptake. The clay reusability was also tested and the outcomes suggested that MC600 had good potential as an economic adsorbent for chromium removal from contaminated water. According to this finding, modified NC is an effective adsorbent for direct Cr(VI) removal from aqueous media and the clay material is signified as an efficient treatment technology can also be adapted to heavy metal removal in wastewater treatment applications and could replace the commercially available adsorbents.

Keywords Clay mineral · Adsorbent · Chromium wastewater · Isotherm modeling

1 Introduction

Nowadays, special attention has been given to wastewater contaminated with heavy metals due to their long-term risk, non-biodegradability and carcinogenic effect. Heavy metals may have the tendency to accumulate in the food chain causing toxicity for the living organisms besides the deterioration to the environment. Choosing an efficient way for managing them is essential to save the ecological system and human health. Chromium is a hard grey steel metal occurring in nature in bound forms and presents 0.1–0.3 mg/kg of the earth's crust [1, 2]. It has several oxidation states, however, the most stable forms are the trivalent (Cr(III)) and hexavalent (Cr(VI)) states. Hexavalent chromium is considered more toxic than the trivalent one since its lethal dose is ranged from 80 to 160 mg/L compared to the dose of 160 to 320 mg/L for the Cr(III) [1, 3].

Currently, as a result of developing advanced technologies and industrialization activities, a global concern is attained regarding the toxic substances [4, 5]. Effluents containing chromium metal are widely discharged from various industrial processes, such as leather industry through tanning and finishing processes, mining and metallurgy [3, 5], textile and dying industries, paper manufacturing, paints, wood preservation, jet aircraft, magnetic tapes, power plants and electroplating [1, 3]. Therefore, for

✉ Maha A. Tony, dr.maha.tony@gmail.com | [1]Chemical Engineering Department, Faculty of Engineering, Minia University, Minya, Egypt. [2]Advanced Materials/Solar Energy and Environmental Sustainability (AMSEES) Laboratory, Basic Engineering Science Department, Faculty of Engineering, Menoufia University, Shebin El-Kom, Egypt.

a sustainable environment these effluents must be treated in an eco-friendly manner to remove chromium ions before being discharged into water bodies [6]. Currently, several methods are available for removing this type of heavy metals from effluent such as membrane separation, flocculation, electrocoagulation and adsorption. However, it is noteworthy to mention that those techniques have the disadvantages of incomplete metal removal, high reagent doses and energy requirements [7, 8].

Many chemical, biological and physical processes have been used for the treatment of wastewater to get rid from toxic pollutants. Some of the physicochemical water treatment methods like flocculation, precipitation, membrane filtration, coagulation, ion exchange, bioremediation, advanced oxidation and adsorption techniques are extensively used for removal of metal ions and other pollutants [9–12]. Among wastewater treatment techniques, the adsorption is one of promising techniques since it is efficient, simple and adsorbents are easily available [10]. In this regard, modified clays proved to be highly efficient adsorbent materials [13]. Generally, adsorption is preferred for its low-cost, abundant, high speed and efficient in removing pollutants besides the simplicity of design and easy in handling [9]. Activated carbon is the most widely applied adsorbent material in wastewater remediation. On the other hand, high cost and also the necessity for regeneration of adsorbent materials are still stand as the main disadvantages for its use [11]. Therefore, recently, with increasing the environmental considerations, searching for new cost-efficient, easy to extract and sustainable adsorbents derived from natural resources that are suitable for adsorption is of interest of many scientists [14].

Modified natural materials that have an improved surface area for efficient adsorption play an important potential for environmental remediation [15]. Such adsorbents include bare palm branches [16] sawdust [17], bagasse [5], orange peel [14], eggshell [18] and clay [11, 19, 20].

From last few years, clay is gaining much attention for its unique characteristics. Clay minerals are signified as layers of mineral silicates that are naturally abundant, inexpensive, non-toxic to the environment, composed of amorphous phase and having different types of geometry [21–23]. It is preferred for its high adsorption capacity, reactivity and stability. The use of clays and clay minerals as natural adsorbents has been previously stated in the literature for removing Orange G dye [24], Direct Red 23 dye [11], phenolic compunds [25], Cr(III) by Kaolin-biofilm [1], copper (II) and Nickel (II) by clay/biopolymer composite [26] from water and wastewater.

To the best of the authors' knowledge, according to the literature published, there is a limited data dealing with the modified natural clay for treating the hexavalent chromium removal from wastewater. In the current investigation the sorption potential of the modified clay prepared from natural one for the removal of hexavalent chromium from aqueous effluents has been explored. The sorption parameters were studied and adsorption isotherm and kinetic models were also applied to describe this adsorption matrix.

2 Materials and methods

2.1 Preparation of clay adsorbent

Natural clay was collected from deposit located near to Minia city in the south of Egypt. The clay is dried in an electric oven at 105 °C for 7 days in order to remove the moisture content at the time of being used. Subsequently, the clay is subjected for a ball mill grinding (1 h) to obtain a fine powder. The resultant clay is referred as (NC) as the native form of clay adsorbent. Thereafter, the clay is introduced for a chemical activation according to the previously reported in literature [27]. The clay is sieved through a 200 mesh and cooked with a 10 M diluted HCl for 90 min with heating (70 °C) and stirring (300 rpm speed). Then, the solution is washed repeatedly using distilled water until the pH of the filtrate is reached to 6.0–7.0. The filtrate is afterwards dried at 70 °C for 5 h. Additionally, the modified clay is subjected to 600 °C for thermally activation through the calcination process and the obtained clay is called MC600.

2.2 Wastewater

To prepare the adsorbate solution, a synthetic solution of chromium-polluted wastewater was synthetically prepared from Cr(VI) (99.9% purity, Sigma-Aldrich, Germany) and used as received without pre-treatment. A stock solution is obtained and different concentrations are further prepared ranged from 2 to 80 mg/L and subjected for treatment.

2.3 Adsorption methodology

To determine the adsorption capacity of the clay mineral adsorbent materials, batch tests were investigated. For the adsorption isotherm studies, the experiments were employed over a concentration ranged from 2 to 60 mg/L of chromium solution at 298 K. A solution of 50 mL of chromium was added to different vessels then the adsorbent dose was further added and the vessels were sealed then subjected for the interaction mixing. Samples were taken at 5, 15, 30, 60, 240 and 24 h for analysis. Subsequently, chromium concentration was determined at the maximum wavelength of Cr(VI) (352 nm) using UV–visible

spectrophotometer (Unico UV-2100 spectrophotometer, USA). The concentration of Cr(VI) are based on the average of three parallel replications. The treatment steps are graphically represented in Fig. 1. It is noteworthy to mention that the remaining chromium in the solution that is only detected is Cr(VI). However, the presence of the less toxic Cr(III) [28] that may be occur in the solution due to the reduction of Cr(VI) into Cr(III) is neglected during the current study.

2.4 Adsorbent characterization

Field-emission scanning electron microscope, SEM micrographs were recorded using a FE-SEM, Quanta FEG 250 with typical magnifications of ×8000 and ×60000. This is accompanied by energy dispersive X-ray spectroscopy (EDX) to analyze the principal composition of the oxides content of the mineral clay. Fourier transform infrared FTIR spectra (Jasco, FT/IR-4100, type A) of the two types of clay minerals were carried out to determine the type of functional group responsible for Cr(VI) adsorption. Brunauer–Emmett–Teller (BET) surface area, S_{BET} was also investigated.

2.5 Isotherm models

There are several types of adsorption mechanism that describing the adsorption process. Langmuir, Freundlich, Temkin and Dubinin–Radushkevich which are the most widely used and accepted isotherms to describe the adsorption process and were applied in the current study.

2.5.1 Freundlich isotherm

Freundlich [29] investigated the Freundlich isotherm model to describe the heterogeneous adsorption surface. The empirical equation of Freundlich isotherm is given by:

$$\ln(q_e) = \frac{1}{n} \ln C_e + \ln K_F \tag{1}$$

where C_e (mg/L) is the chromium concentration at equilibrium, q_e (mg/g) is the equilibrium adsorption capacity, n is the dimensionless heterogeneous constant that related to the adsorption intensity and K_F (L/g) is the Freundlich constant that related to adsorption capacity. The dimensionless constant n gives an indication of how the adsorption is favourable. When 1/n is greater than unity, it represents a favorable adsorption conditions [30].

2.5.2 Langmuir isotherm

Langmuir [30] isotherm model describes the adsorption system as a monolayer adsorption process on a homogeneous surface. The model-linearized equation is given as the following:

$$\frac{C_e}{q_e} = \frac{1}{K_L} + \frac{a_L}{K_L} C_e \tag{2}$$

Fig. 1 Schematic representation of the steps of clay preparation and the adsorption process
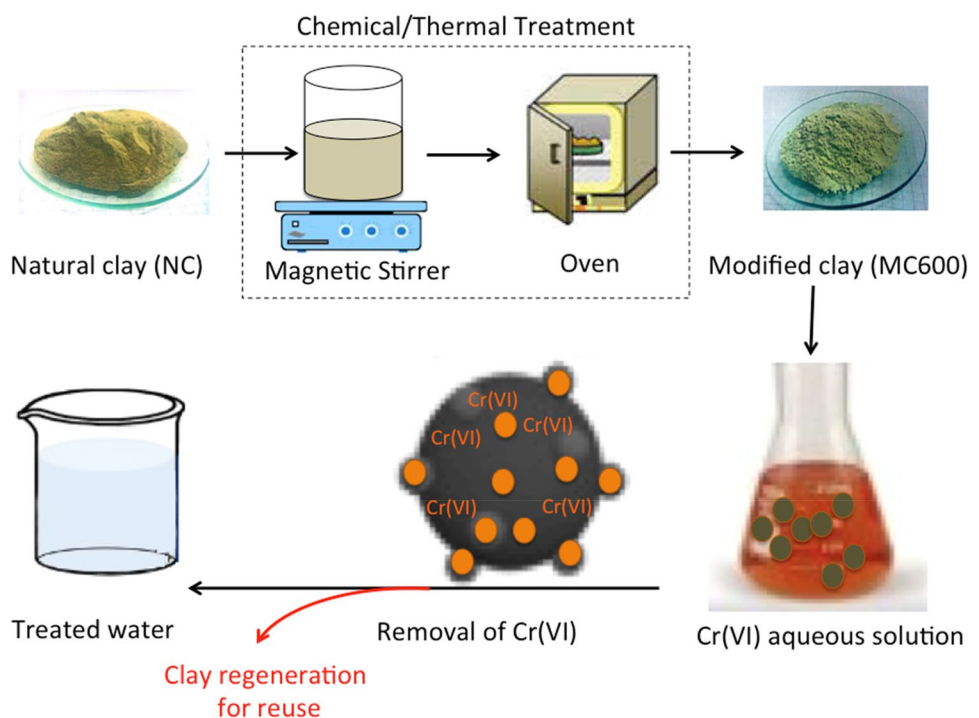
$$Q_o = \frac{K_L}{a_L} \tag{3}$$

where K_L and a_L ate the Langmuir constants related to binding sites affinity and adsorption energy. Q_o is the monolayer adsorption capacity of the mass of chromium per unit mass of clay (mg/g).

2.5.3 Temkin isotherm

Temkin isotherm model [31] describes the indirect effect of adsorbent/adsorbate interactions on the adsorption process. It estimates the heat of the layer adsorption is in a linear decrease as a result of increase in surface coverage. This isotherm model is only valid at an intermediate range of ion concentrations. The linear expression of the Temkin equation is represented as Eq. (4):

$$q_e = B \ln K_T + B \ln C_e \tag{4}$$

where B is expressed as ($B = \frac{RT}{b}$) and is related to the heat of adsorption, T is the absolute temperature (298 K), R is the universal gas constant (8.314 J mol^{-1} K^{-1}) and K_T is the equilibrium binding constant.

2.5.4 Dubinin–Radushkevich (D–R) isotherm

D–R isotherm is limited to a monolayer and can be applied to investigate the energy of adsorption onto a heterogeneous surface [30, 32]. The linearized form is shown in Eq. (5):

$$\ln q_e = \ln q_s - K_{DR}\varepsilon^2 \tag{5}$$

where q_s is the monolayer saturation capacity (L/g) and K_{DR} is the constant of Dubinin–Radushkevich adsorption energy, which gives the mean free energy (E) of sorption per molecule of the sorbate and can be estimated from the relationship of $E = \frac{1}{\sqrt{2K_{DR}}}$. ε is denoted as isotherm constant and it is given by: $\varepsilon^2 = RT\ln\left(1 + \frac{1}{C_e}\right)$.

The model was used to investigate the chemical and physical adsorptions of chromium ions with its mean free energy and this is estimated from the calculated E value.

2.6 Kinetic models

The most popular kinetic models, Lagergren's pseudo-first-order and pseudo-second-order were applied to fully investigate the adsorption mechanism and the rate controlling steps of chromium adsorption process.

2.6.1 Lagergren's pseudo-first-order kinetic model

Lagergren's model assumes that one chromium molecule of adsorbate is being adsorbed by one sorptive site in the clay adsorbent material [30]. The linearized form of the model of Lagergren is given as the following equation:

$$\log\left(q_e - q_t\right) = \frac{K_1}{2.303}t + \log(q_e) \tag{6}$$

where q_t (mg/g) is amount of the chromium adsorbed at time (t) and K_1 is the pseudo-first order rate constant of chromium adsorption onto clay mineral.

2.6.2 The pseudo-second-order kinetic model

The pseudo-second-order supposes the occupation rate of sorption sites is proportional to the square number of vacant sites and it can be expressed as the following equation [33]:

$$\frac{t}{q_e} = \frac{1}{K_2 q_e^2} + \frac{1}{q_e}t \tag{7}$$

where K_2 is the pseudo-second order adsorption rate constant.

3 Results and discussion

3.1 Characterization of mineral clay

3.1.1 FTIR spectroscopy

Fourier transform infrared (FTIR) transmittance spectrum analysis is useful to identify the various forms of minerals existing in the clay. The two types of clay mineral adsorbents, NC and MC600 were analysed using FTIR techniques and the data are shown in Fig. 2a, b. The IR studies of natural clay (NC) is shown in Fig. 2a. Although, there are main absorption intensive bands for clay besides the coupled vibrations are appreciable due to the availability of various constituents. The absorption band at 781.9 cm^{-1} is assigned for the O–H stretching vibration of structural water. The Si–O stretching vibrations (silanol) are identified at 462.8 cm^{-1}, 528.4 cm^{-1}, 781.9 cm^{-1} and 1032.6 cm^{-1} that representing the presence of quartz [34, 35]. Additionally, the appearance of (Si–O–Si) band at 1032.6 cm^{-1} also confirms the presence of quartz [34]. The bands at 528.4 cm^{-1}, 1638.2 cm^{-1}, 3438.4 cm^{-1} and 3694.9 cm^{-1} indicate the possibility of the hydroxyl linkage. Nonetheless, the bands at 1638.2 cm^{-1} and 3438.4 cm^{-1} in the clay spectrum of clay material suggests the possibility of water
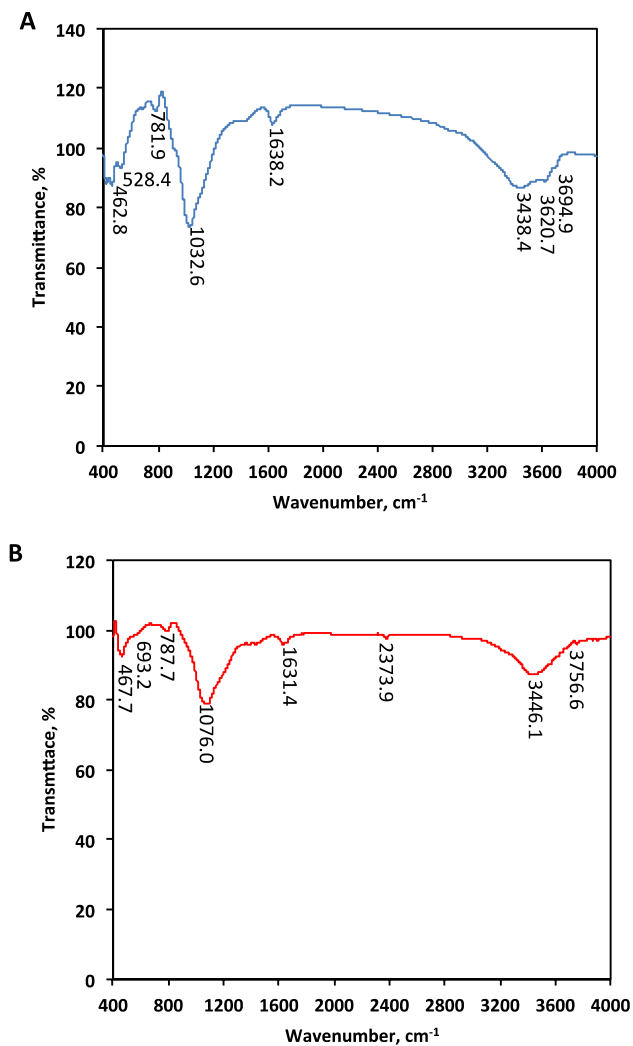
Fig. 2 FTIR spectrum of the mineral clay **a** NC and **b** MC600

of hydration in the clay mineral. The inter layer hydrogen bonding in the natural clay (NC) is characterized at the band assigned at 3620.7 cm^{-1}. Most of the bands observed at 462.8 cm^{-1}, 528.4 cm^{-1}, 781.9 cm^{-1}, 1638.2 cm^{-1}, 3438.4 cm^{-1}, 3620.7 cm^{-1} and 3694.9 cm^{-1} illustrate the existence of kaolinite [36]. The bands at 462.8 cm^{-1} are reflecting the indication of presence Si–O–Fe [37]. In addition, clay mineral spectra show bands at 528.4 cm^{-1} and 781.9 cm^{-1} related to the stretching vibrations of Si–O–Al group [34], which may demonstrate the presence of illite [38]. The band 1032.6 cm^{-1} confirms the presence of illite. The band near 781.9 cm^{-1} attributes the presence of Al–Mg–OH bonding, this spectrum demonstrates the possibility of the presence of montmorillonite [39].

As noted from Fig. 2b that shows the IR absorption spectra of the modified clay (MC600), there is a shift in absorption bands. The change in the absorption band of –OH group from 3694.9 to 3756.6 cm^{-1} vibrating

band illustrates the role of the acid activation on shifting the –OH band. This indicates that the acid activation of the mineral clay attributing the protons penetration into the clay layer, which is responsible on attacking the OH groups causing alterations in the adsorption bands [40]. The change in the absorption band of H–O–H (from 1638.2 and 34,382 cm^{-1} to 1631.4 cm^{-1} and 2446.1 cm^{-1}, respectively) indicates the acid activation affected the clay on this position. Additionally, the acid activation of the clay presenting the presence of a new signal band of absorption at 2372.9 cm^{-1} that assigned to the S–H stretching vibration. Furthermore, there is a change in the Si–O stretching bands from the natural to the modified clay, which confirms the role of the acid activation on the position of those bands. Hence, the FTIR results are quite helpful for identifying the different minerals' forms that present in the introduced adsorbents.

3.1.2 SEM, EDX and S_{BET}

3.1.2.1 SEM In order to investigate the structure of both the NC and MC600, the morphology of both adsorbents were characterized using SEM images at different magnifications. Figure 3a–d shows that both types of mineral clay are characterized by irregular layered structure that has a smooth surface. The native clay SEM images (Fig. 3a, b) representing large agglomerates of irregular shape particles. A considerable smaller in size particles with constituted of disordered aggregates for the chemically-thermally treated clay (Fig. 3c, d). A significant decrease in the particle size from the range of 1.34–5.688 μm of the unmodified clay to the range 1.073–1.949 μm and 616.9–897.7 nm for the modified clay is recognized.

The surface is described with the presence of a lot of asymmetric open pores. Some textural changes in the external surface of the clay, which suggest changes in their porosity is achieved. Thus, MC600 exhibits more porosity than the native clay. The native clay has few voids compared to the modified one that is due to the activation with HCl followed by the carbonization increases the size of the pores as well as decomposes the volatile organic matters in the clay.

Based on these results, it is reasonable to conclude that the chemical-thermal treatment promotes the formation of disordered and less cohesive aggregates, may be due to a reduction in the clay molecules interactions. This change constitutes an important advantage considering for adsorption applications. Hence, this helps the chromium molecules to simply disperse into the modified clay more than the native one and increases the adsorption capacity of MC600.
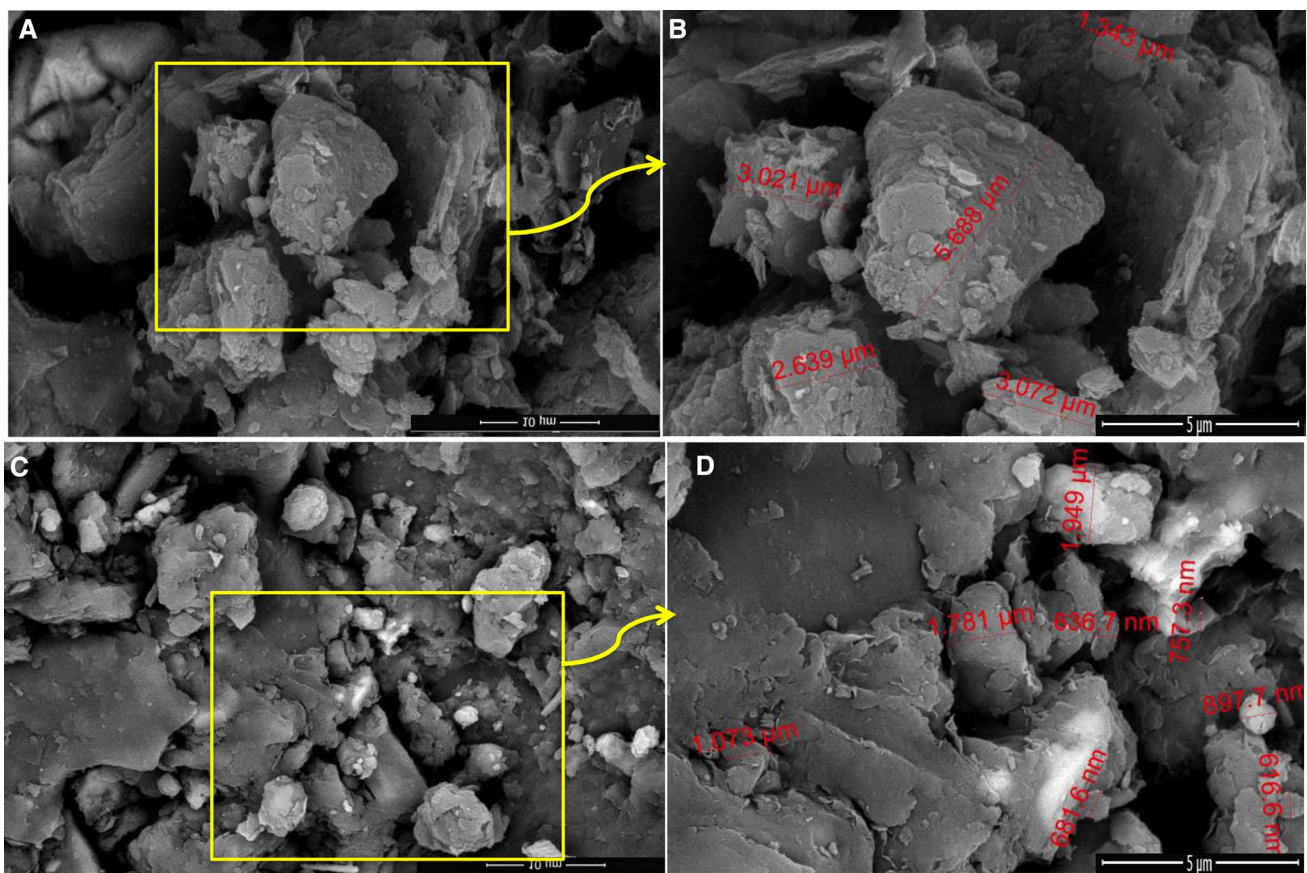
Fig. 3 Morphological structure (SEM image) of (**a**, **b**) natural clay (NC) and (**c**, **d**) modified clay (MC600) at different magnifications

**Table 1** EDX elemental analysis results of natural clay (NC) and modified clay (MC600)

Element	Weight %	
	NC	MC600
SiO_2	64.37%	81.81%
Al_2O_3	12.63%	11.16%
Fe_2O_3	7.55%	3.26%
CaO	4.37%	0.90%
MgO	1.84%	0.59%
K_2O	1.26%	1.04%
Na_2O	1.50%	0.18%
SO_3	0.09%	0.10%
LOI	6.39%	0.96%

3.1.2.2 EDX Elemental analysis techniques for the natural mineral clay sample and the modified mineral clay that is chemically-thermally treated are given using Energy Dispersive X-ray analyzer (EDX). The results given in Table 1 illustrate the chemical composition of both clays from different oxides. SiO_2 is being the major component in the both clay samples. As seen from Table 1, the percentage of SiO_2 is higher in MC600 than the corresponding oxides in the NC. Besides the presence

of Al_2O_3 and Fe_2O_3 in the both samples with a slightly change.

Previous studies [41–43] have motioned the importance of the oxides of SiO_2, Al_2O_3 and Fe_2O_3 particles in improving the tendency of adsorption. These oxides have reactive groups that interact with the adsorbate and thus increase the adsorption capacity [41].

3.1.2.3 S_{BET} According to the result obtained from Brunauer–Emmett– Teller ssurface area (S_{BET}) analysis, the specific surface area of natural and modified clays are 34 and 136 $m^2\ g^{-1}$, respectively. This data clarifies the effect of the chemical and thermal modification of the clay. The value of the S_{BET} for the modified bagasse is notably higher than that of the natural clay which is related to the thermally and chemically treatment effect on the particle size of the clay. These results confirm the observed modifications indicated in the SEM images.
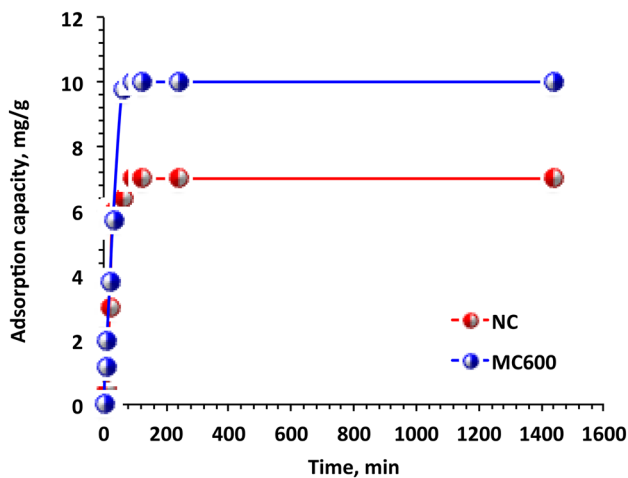
Fig. 4 Effect of contact time on the adsorption capacity (Chromium concentration 30 mg/L; adsorbent dose 1.0 g/L and 298 K)

3.2 Adsorption capacity

### 3.2.1 Chromium adsorption related to contact time

Initially, the contact equilibrium time of adsorption process should be examined to establish the adsorption matrix of chromium onto the clay surface. The adsorption time related to the chromium adsorption is graphically represented in Fig. 4. The results indicate that for both types of clay minerals (NC and MC600), the adsorption rate of chromium is increased with increasing the contact time.

The adsorption process took place during two stages, the initial stage where there was a rapid uptake followed by a steady stage uptake. The adsorption equilibrium was established in 90 min of contact time between the aqueous chromium solution and the clay mineral. Afterwards, no further change in the adsorption process. This could be attributed by the saturation of adsorption sites. However, rapid chromium adsorption in the initial stage is due to the high initial Cr(VI) concentration on the adsorbate and the corresponding available vacant sites on the clay mineral adsorbent materials [16, 44, 45]. The final adsorption capacities of Cr(VI) from aqueous solution using NC and MC600 are 7.0 and 10.0 mg/g, respectively. It is noted that the modified clay has high adsorption capacity this is due to the abundance of available adsorption sites and the increase in the surface area (as seen in Fig. 4) due to the acid activation process. These results are in accordance with that previously reported by Mahvi and Dalvand [11] in treating dye solution using nanoclay adsorbent materials. For practical applications, it is significant to state that the final effluent may be contain trace amounts of Cr(III) due to the reduction of Cr(VI) which may be need a further precipitation before the final disposal of the effluent.

3.2.2 Effect of initial chromium concentration on adsorption capacity

The effect of initial Cr(VI) concentration on the adsorption technique is carried out for 90 min at 298 K using 0.1 g of clay and the results for both adsorbents are presented in Fig. 5. The Cr(VI) solutions has an initial concentrations ranged from 10 to 80 mg/L. It is noted from the results that for both adsorbents, NC and MC600, increasing the hexavalent chromium concentration results in a significant improve in the adsorption capacity. This positive linear relationship between the adsorption capacity and chromium concentration signifies that the adsorption capacity could be further improved by continue increasing the chromium concentration. The adsorption capacity increases from 1.1 to 4.0 mg/g with increasing the chromium concentration from 10 to 80 mg/L, respectively. However, the removal efficiency decreases from 12 to 5% with the increase in the Cr(VI) concentration from 10 to 80 mg/L using NC and from 10 to 3.7% using MC600 adsorbent.

These result could be explained by the fact that the number of adsorption sites on a specific amount of adsorbent are limited [16, 46]; therefore, with increasing the number of chromium molecules, the number of active sites on the adsorbent are not enough to adsorb all chromium molecules uptake and, consequently, the removal efficiency decreases. However, with increasing the initial Cr(VI) concentration from 10 to 80 mg/L, the amount of chromium adsorbed onto the adsorbent clay minerals is increased. This could be due to an increase in the concentration gradient between Cr(VI) molecules in the solution and Cr(VI) molecules on the adsorbent surface at higher
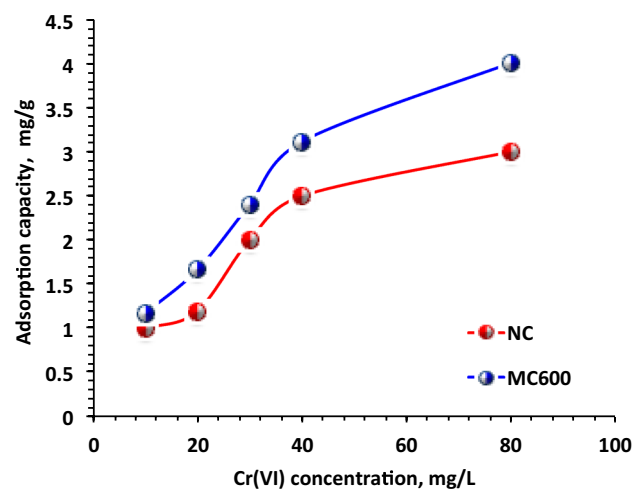
Fig. 5 Effect of initial chromium concentration on adsorption capacity (adsorbent dose 0.1 g/L; 500 rpm and 298 K)

initial Cr(VI) concentrations causes an increase in the driving force and adsorption capacity [11].

3.2.3 Evaluating the adsorption parameters

In order to determine the best adsorption conditions for optimum sorption matrix for both natural and modified clay minerals, the different adsorption parameters are investigated.

3.2.3.1 Effect of mixing rate The effect of mixing rate is varied from 100 to 600 rpm on the chromium adsorption using a 30 mg/L of chromium initial concentration and the results are displayed in Fig. 6a at constant temperature 298 K and 2.3 g of clay dose. As seen from Fig. 6a, increasing the mixing rate from 100 to 500 rpm, the adsorption capacity varied from 0.45 to 2.2 mg/g, respectively for the clay adsorbent. This could be due to the increase in the adsorbate/adsorbent mixing rate that is enhancing the suspension and deagglomeration of particles. Thus, increasing the solid–liquid interface contact and hence improving the chromium molecules transfer onto the sorption sites. However, it is clear from the results that further increase in the agitation speed more than 500 rpm, results in a decrease in the adsorption capacity. This decrease may be attributed to an increase in the desorption tendency of the chromium molecules. The high agitation speed is causing more input energy and higher shear force which results in breaking down the bonds between the Cr(VI) and the clay adsorbent. Thus, the result may be an increase in the tendency of desorption of Cr(VI) [47]. Therefore, 500 rpm is a sufficient agitation speed to assure that binding sites of the adsorbent surface are available for chromium uptake.

3.2.3.2 Effect of adsorbent dose The effect of different dosages of clay adsorbents on adsorption capacity is presented in Fig. 6b. For both types of mineral clay adsorbents, increasing the adsorbent dose results in an improvement in the adsorption capacity. The maximum adsorption capacity for both adsorbents, natural clay (NC) and modified clay (MC600), that is corresponding to 0.5 g/L clay are 4.5 and 7.0 mg/g, respectively. However, with further increase in the clay concentration, the adsorption capacity decreases again to 2.0 and 2.6 mg/g for NC and MC600, respectively when increasing the clay dose to 3.3 g/L. This could be attributed by the utilization rate of the clay mineral adsorbent is reduced since the adsorbent dose is a reversible relation between the unit adsorption capacities. Furthermore, the high clay mineral dose affects the adsorbent aggregation, which decreases the available adsorption active sites as the overall surface area is reduced. This aggregation phenomenon decreases
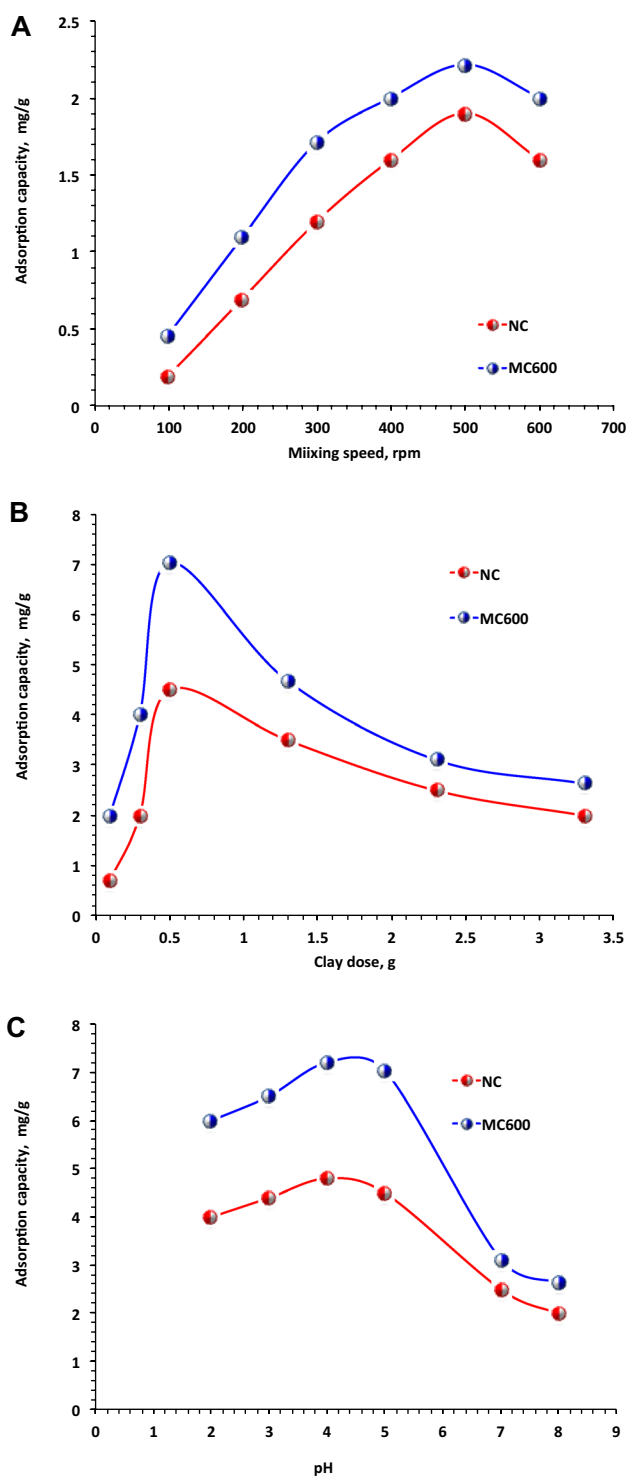
Fig. 6 Effect of operating parameters on adsorption capacity **a** effect of mixing speed; **b** effect of adsorbent dose and **c** effect of pH (Chromium concentration 30 mg/L and 298 K)

the total available surface area that is utilized for the adsorption process and the result is a decrease in the adsorption capacity [18]. These results are in agreement

with that previously stated in the literature in dye removal using hen feather as an adsorbent material [48].

3.2.3.3 Effect of pH pH is considered one of the decisive factors affecting the adsorption process. pH is controlling the surface charge of the clay adsorbent materials, the adsorption availability of the chromium and the ionization degree of the molecules in the aqueous media [49, 50]. The initial chromium solution pH on the adsorption capacity is evaluated at various pH ranged from 2.0 to 8.0 is shown in Fig. 6c.

As noted in the Fig. 6c, by increasing pH from 2.0 to 5.0 an increase in the adsorption capacity is achieved for both types of adsorption that is reached to 4.5 and 7.0 mg/g for NC and MC600, respectively. However, further increase in the pH value, a decrease in the adsorption capacity is observed. This could be illustrated by, at low pH value (2.0), the surface of the clay adsorbent materials is positively charged. Si–O (silanol) and Si–O–Al active groups on the clay surface are surrounded by hydronium ions and protonated due to the presence of excess H^+ in the solution. Thereby, blocking the metal ions from binding sites on the clay adsorbent and this is not favour for the positively charged chromium metal adsorption. However, by increasing the solution pH, the deprotonation mechanism of the active groups is occurred and this attributed to a decrease in the number of positively charged sites on the clay adsorbent. Hence, Cr(VI) adsorption from aqueous solution is preferred due to the increasing of the electrostatic attractive interactions between the clay surface and the chromium ions in the solution [1, 44]. However, further increase in the solution pH that results in a reduction in the chromium uptake. This could be due to the loss of the active sites of the adsorbent material [30, 32]. Additionally, at the high solution pH, the chemical interaction occurs between the chromium ions and the OH_2 ions existing in aqueous media that causing hydrolysis on metal ions that may cause a precipitation of chromium in the form of hydroxide speciation. Thus the overall adsorption capacity is decreased at the high pH value [51, 52].

Comparison of the sorption capacities of the mineral clay material with various adsorbents from the literature for adsorbing chromium metal is tabulated in Table 2. Certainly, the adsorption capacities of mineral clay adsorbents (NC and MC600) in comparable to the different adsorbents listed in the table demonstrate a reasonable adsorption capacity of the chromium uptake. Nevertheless, it is observed that there are other adsorbents with promising adsorption capacities. However, it should be mention the other considerations such as the adsorbents are considered as chemical composite from different materials with chemical compounds. Furthermore, the type of chromium metal and the solution concentration may also affect the adsorption uptake.

3.3 Adsorption isotherm models

In order provide detailed information for getting a comparison of the two adsorbent materials for a large scale applications, investigation of the equilibrium data and the maximum adsorption capacity of the adsorbent are very useful. Adsorption isotherms were generated for chromium adsorption onto the two types of mineral clay materials and applied for different isotherm models. Series of adsorption isotherm models: Langmuir, Frendlich, Temkin and Dubinin–Radushkevich are investigated for hexavalent chromium adsorption matrix and the data is shown in Fig. 7 and tabulated in Table 3.

It is noted from the data in Table 3, the value of the linear correlation coefficient, R^2, is at a range from 0.96 to 0.97 for Freundlich isotherm. Thus, the adsorption matrix is a heterogeneous surface condition. Further, the values of 1/n are found to be less than 1 indicating that the adsorption of chromium is favourable uptake [30]. Also, this low 1/n value signifies a chemisorption. Further, the K_F values are low which suggests that there was low uptake of the chromium ions onto the clay surface process [44]. This finding is similar to another study [1] on the sorption of chromium using other adsorbent materials. However, Huang et al. [53] found the chromium removal is following

Table 2 Comparison of adsorption capacities of various adsorbents with the current study for Chromium metal removal

| Adsorbent	Chromium metal	Adsorption capacity, mg/g	Isotherm time	T, K	References
NC	Cr(VI)	7.0	90 min	298	Current study
MC600	Cr(VI)	10.0	90 min	298	Current study
Aluminium oxide	Cr(III)	3.36	60 min	298	[12]
Groundnut shell	Cr(VI)	3.6	120 min	338.5	[42]
Kaolin-supported biomass	Cr(III)	14.53	48 h	313	[47]
Ammonium chloride chitosan–bentonite	Cr(VI)	22.17	30 min	298	[15]
Carboxymethyl cellulose	Cr(VI)	6.53	10 h	298	[54]
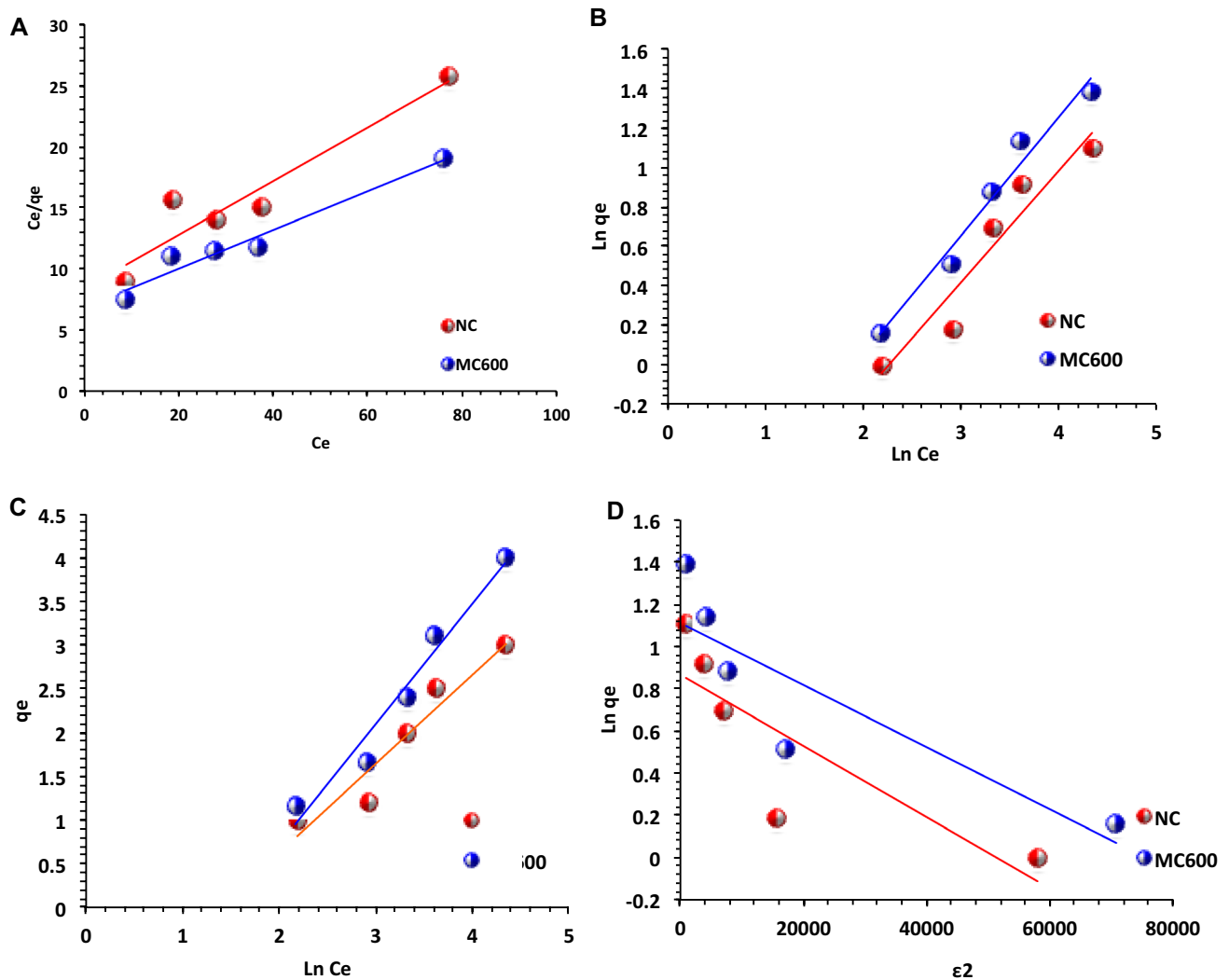
Fig. 7 Adsorption isotherm models for hexavalent chromium removal from aqueous media **a** Langmuir, **b** Frendlich, **c** Temkin and **d** D–R models

the Langmuir isotherm model using ammonium chloride chitosan–bentonite as an adsorbent material. Additionally, Bayuo et al. [44] reported that the chromium adsorption onto groundnut shell material is well fitted with Temkin isotherm compared to the other isotherm models tested.

3.4 Kinetics of adsorption

Kinetic study is considered significant features that represent the adsorption techniques. In order to assess the adsorption efficiency of adsorbent materials introduced in this study with the contact time, two kinetic adsorption models of the Lagergren's pseudo-first-order and pseudo-second-order equations are applied. The linear plot of the two models according to Eqs. (6) and (7) are explored (as seen in Fig. 8) and the comparative data (Table 4) of the two models are analyzed. The results computed in Table 4

indicate that the data is well fitted to the pseudo-second-order kinetic model according to the values of correlation coefficients (R^2 0.99). Similar phenomenon has been observed previously in the adsorption of reactive dye using bagasse adsorbent [54].

3.5 Adsorbent reusability

After treatment, the modified clay at 600 °C (MC600) adsorbent was washed out for reuse in order to investigate its cyclic performance and treatment efficiency. In this regard, 0.5 M HCl was used for clay regeneration then the clay is submitted for successive use after regeneration. The outcome of this work is illustrated in Fig. 9. The regenerated MC600 revealed a slight decrease after five cycles from 66 to 59% as seen in Fig. 9. Hence, the clay material showed a good reusability potential since

Table 3 Equilibrium parameters of isotherm models for Cr(VI) adsorption onto clay

| Isotherm	Parameters	NC	MC600
Langmuir	a_L, L/mg	0.03	0.02
	K_L	0.12	0.15
	Q_o, mg/g	4.56	6.32
	R^2	0.89	0.96
Freundlich	K_F	1.92	0.32
	$1/n$	0.57	0.60
	R^2	0.96	0.97
Temkin	B, J/mol	1.02	1.38
	A, L/g	0.25	0.23
	R^2	0.92	0.96
D–R	q_m, mol/g	2.38	2.04
	$K_{D-R} \times 10^{-5}$, mol²/J²	2.00	1.00
	$E \times 10^{-6}$, kJ/mol	3.47	3.12
	R^2	0.69	0.75

**Table 4** Kinetic models parameters for chromium adsorption by clay mineral adsorbents

Model parameters	NC	MC600
Lagergren's Pseudo-first-order		
q_e (mg g^{-1}) $\times 10^{-2}$	88.33	117.92
K_1 (min^{-1}) $\times 10^{-2}$	5.58	6.45
R^2	0.89	0.90
Pseudo-second-order		
q_e (mg g^{-1})	7.14	10.16
K_2 (g mg^{-1} min^{-1}) $\times 10^{-2}$	0.61	0.52
R^2	0.99	0.99

its successfully eluted chromium ions from aqueous media. After successive cycles of adsorption–desorption test the results suggested that the clay material is outstanding recycling adsorption material. Thus, this making chromium removal from aqueous effluent with natural clay is a more sustainable and economical alternative. This slight decrease in the removal efficiency could be illustrated by the occupation of active sites by chromium metal that covered the active centers and therefore preventing them from adsorbing more molecules. Likewise Pan et al. [55] investigated the same trend in organics adsorption from wastewater.

4 Conclusion

The present investigation is reported on the application of a naturally abundant clay mineral materials as an adsorbents for removing hexavalent chromium Cr(VI) ions from the wastewater matrix. The experimental results revealed that the equilibrium isotherm time is reached at 90 min and increasing the adsorbent dose, pH and the agitation speed till certain limits increases the adsorption capacity. The adsorbent dose of 0.5 g-clay/L of solution and the solution pH of 5.0 are corresponding to the maximum chromium removal. This study is also dealt with comparing the sorption capacity of the natural and modified clay mineral, which showed adsorption capacity of 10.0 and 7.0, respectively. Furthermore, the equilibrium sorption data was fitted well with the Frendlich isotherm model. Also, kinetic studies was investigated and revealed that the chromium removal onto
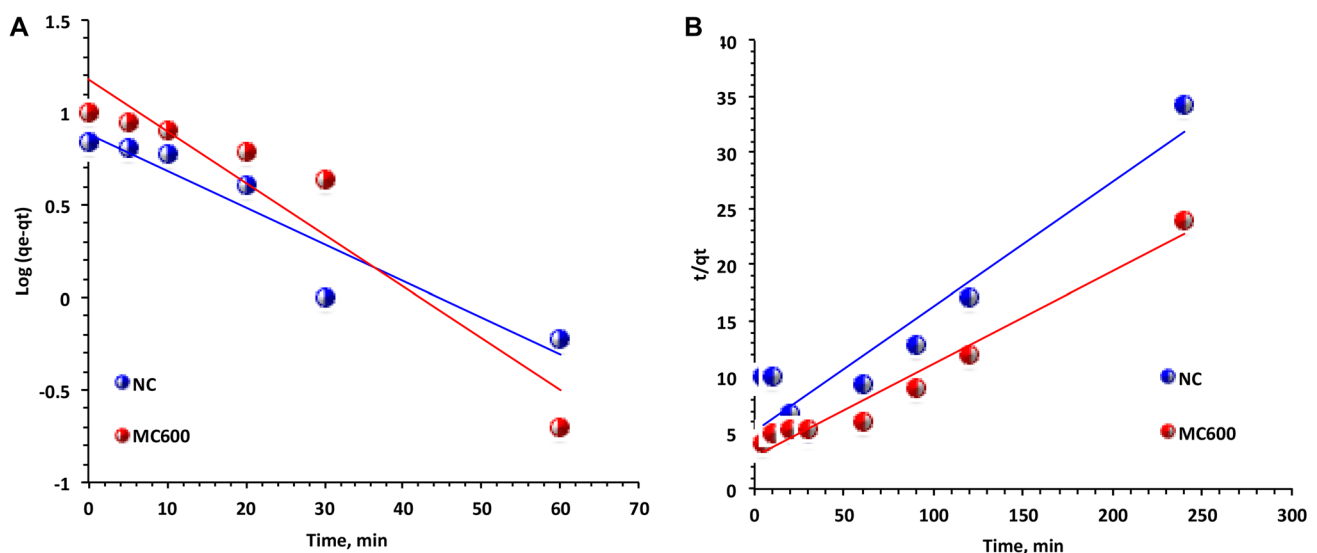
Fig. 8 Kinetic modelling plot of chromium adsorption **a** first order kinetics and **b** second order kinetics
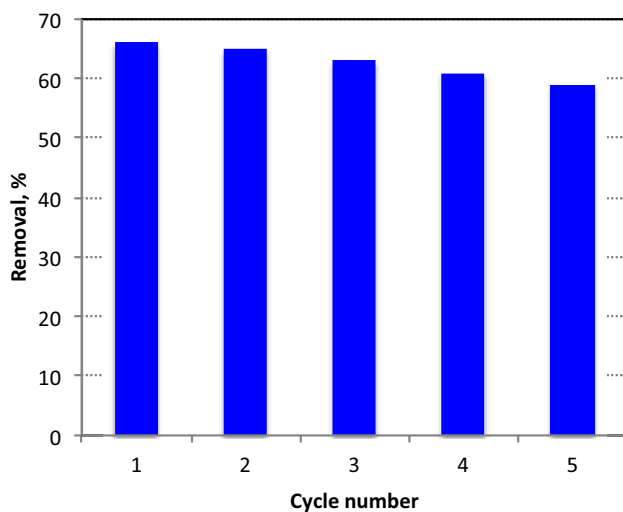
Fig. 9 Regeneration and reuse of modified clay for Chromium removal

adsorbent is following the pseudo-second-order kinetic model. This investigation introduces an economical, easily available adsorbent for the removal of chromium ions from the aqueous media.

Compliance with ethical standards

Conflict of interest The author declares that there is no conflict of interest.

References

1. Fathima A, Rao JR, Nair BU (2012) Trivalent chromium removal from tannery effluent using kaolin-supported bacterial biofilm of Bacillus sp isolated from chromium polluted soil. J Chem Technol Biotechnol 87:271–279
2. Tony MA, Zhao YQ, El-Sherbiny MF (2011) Fenton and fenton-like AOPs for alum sludge conditioning: effectiveness comparison with different Fe^{2+} and Fe^{3+} salts. Chem Eng Commun 198(3):442–452
3. Akar ST, Yetimoglu Y, Gedikbey T (2009) Removal of chromium (VI) ions from aqueous solutions by using Turkish montmorillonite clay: effect of activation and modification. Desal 244(1–3):97–108
4. Tayeb AM, Farouq R, Mohamed OA, Tony MA (2019) Oil spill clean-up using combined sorbents: a comparative investigation and design aspects. Int J Environ Anal Chem. https://doi.org/10.1080/03067319.2019.1636976
5. Tony MA (2020) Zeolite-based adsorbent from alum sludge residue for textile wastewater treatment. Int J Sci Technol. https://doi.org/10.1007/s13762-020-02646-8
6. Giraldo L, Rodriguez-Estupina P, Moreno-Piraja JC (2019) Isosteric heat: comparative study between clausius–clapeyron, CSK and adsorption calorimetry methods. Processes 7:203–228. https://doi.org/10.3390/pr7040203
7. Tony MA, Purcell PJ, Zhao YQ, Tayeb AM, El-Sherbiny MF (2015) Kinetic modeling of diesel oil wastewater degradation using photo-Fenton process. Environ Eng Manag J14(1):11–16
8. Zhao YQ, Keogh C, Tony MA (2009) On the necessity of sludge conditioning with non-organic polymer: AOP approach. J Res Sci Technol 6(3):151–155
9. Dalvand A, Khoobi M, Nabizadeh R, Ganjali MR, Gholibegloo E, Mahvi AH (2018) Reactive dye adsorption from aqueous solution on HPEI-modified Fe_3O_4 nanoparticle as a superadsorbent: characterization, modeling, and optimization. J Polym Environ 26(8):3470–3483
10. Mahvi AH (2008) Application of agricultural fibers in pollution removal from aqueous solution. Int J Environ Sci Technol 5(2):275–285
11. Mahvi AH, Dalvand A (2019) Kinetic and equilibrium studies on the adsorption of Direct Red 23 dye from aqueous solution using montmorillonite nanoclay. Water Qual Res J. https://doi.org/10.2166/wqrj.2019.008
12. Tony MA, Parker H, Clark JH (2016) Treatment of laundrette wastewater using Starbon and Fenton's reagent. J Environ Sci Health A 51(11):974–979
13. Kasina M, Wendorff-Belon M, Kowalski PR, Michalik M (2019) Characterization of incineration residues from wastewater treatment plant in Polish city: a future waste based source of valuable elements? J Mater Cycles Waste Manag 21:885–896
14. Arami M, Limaee NY, Mahmoodi NM, Tabrizi NS (2005) Removal of dyes from colored textile wastewater by orange peel adsorbent: equilibrium and kinetic studies. J Colloid Interface Sci 288(2):371–376
15. Tony MA, Parker H, Clark JH (2019) Evaluating Algibon adsorbent and adsorption kinetics for launderette water treatment: towards sustainable water management. Water Environ J 33(3):401–408
16. Ashour EA, Tony MA, Purcell PJ (2014) Use of agriculture-based waste for basic dye sorption from aqueous solution: kinetics and isotherm studies. Am J Chem Eng 2(6):92–98
17. Hebeish A, Ramadan M, Abdel-Halim E, Abo-Okeil A (2011) An effective adsorbent based on sawdust for removal of direct dye from aqueous solutions. Clean Technol Environ Policy 13(5):713–718
18. Ashour EA, Tony MA (2017) Equilibrium and kinetic studies on biosorption of iron (II) and iron (III) ions onto eggshell powder from aqueous solution. Appl Eng 1(3):65–73. https://doi.org/10.11648/j.ae.20170103.13
19. Kausar A, Shahzad R, Iqbal J, Muhammad N, Ibrahim SM, Iqbal M (2020) Development of new organic-inorganic, hybrid bionanocomposite from cellulose and clay for enhanced removal of Drimarine yellow HF-3GL dye. Inter J Biol Macromol 149:1059–1071
20. Moharami S, Jalali M (2013) Removal of phosphorus from aqueous solution by Iranian natural adsorbents. Chem Eng J 223:328–339
21. Jamshidi A, Rafiee M, Rad MJ (2014) Adsorption behavior of reactive blue 29 dye on modified nanoclay. Trend Appl Sci Res 9(6):303
22. Hu B, Ai Y, Jin J, Hayat T, Alsaedi A, Zhuang L, Wang X (2020) Efficient elimination of organic and inorganic pollutants by biochar and biochar-based materials. Biochar 2:47–64. https://doi.org/10.1007/s42773-020-00044-4
23. Niroumand H, Zain M, Alhosseini SN (2013) The influence of nano-clays on compressive strength of earth bricks as sustainable materials. Procedia Soc Behav Sci 89:862
24. Salam MA, Kosa SA, Al-Beladi A (2017) Application of nanoclay for the adsorptive removal of Orange G dye from aqueous solution. J Mol Liq 241:469–477
25. Nayak PS, Singh BK (2007) Removal of phenol from aqueous solutions by sorption on low cost clay. Desal 207:7

26. Malayoglu U (2018) Removal of heavy metals by biopolymer (chitosan)/nanoclay composites. Sep Sci Technol. https://doi.org/10.1080/01496395.2018.1471506

27. Sirait M, Bukit N, Siregar N (2017) Preparation and characterization of natural bentonite into nanoparticles by coprecipitation method. In: AIP conference proceedings, vol 1801. https://doi.org/10.1063/1.4973084

28. Ding J, Pu L, Wang Y, Wu B, Yu A, Zhang X, Pan B, Zhang O, Gao G (2018) Adsorption and reduction of Cr(VI) together with Cr(III) sequestration by polyaniline confined in pores of polystyrene beads. Environ Sci Technol. https://doi.org/10.1021/acs.est.8b02566

29. Freundlich H (1906) Over the adsorption in solution. J Phys Chem 57:470

30. Parker HL, Budarin VL, Clark JH, Hunt AJ (2013) Use of starbon for the adsorption and desorption of phenols. ACS Sustain Chem Eng 1:1311

31. Ringot D, Lerzy B, Chaplain K, Bonhoure J, Auclair E, Larondelle Y (2007) In vitro biosorption of ochratoxin A on the yeast industry by-products: comparison of isotherm models. Bioresour Technol 98(9):1812–1821

32. Tony MA (2020) Central composite design optimization of Bismarck Dye oxidation from textile effluent with Fenton's reagent. Appl Water Sci 10:108. https://doi.org/10.1007/s13201-020-01192-5

33. Qin J, Qiu E, Rong X, Yan J, Zhao H, Yang D (2014) Removal of basic fuchsin dye from aqueous solutions using graphite oxide modified aromatic polyurethane foam material. Toxicol Environ Chem 96(6):849

34. Bukalo NN, Ekosse GE, Odiyo JO, Ogola JS (2017) Fourier transform infrared spectroscopy of clay size fraction of cretaceous-tertiary kaolins in the Douala sub-basin, Cameroon. Open Geosci 9:407

35. Marel HV, Bentelspacher H (1976) Atlas of infrared spectroscopy of clay minerals and their admixtures. Elsevier Science Publishers, New York

36. Tuddenham WM, Lyon R (1960) Infrared techniques in the identification and measurement of minerals. Anal Chem 32:1630

37. Ahangaran F, Hassanzadeh A, Nouri S (2013) Surface modification of $Fe_3O_4@SiO_2$ microsphere by silane coupling agent. Int Nano Lett 3:23–27

38. Tiniti A, Tugnoli V, Bonora S, Francioso O (2015) Recent applications of vibrational mid-Infrared (IR) spectroscopy for studying soil components: a review. J Central Eur Agric 16(1):1

39. Vaculikova L, Plevova E (2005) Identification of clay minerals and micas in sedimentary rocks. Acta Geodynamica et Geomaterialia 2(138):167–175

40. Ozcan AS, Erdem B, Ozcan A (2005) Adsorption of acid blue 193 from aqueous solution onto BTMA activated bentonite. Colloid Surf A 266:73–81

41. Mosallanejad S, Dlugogorski BZ, Kennedy EM, Stockenhuber M (2018) On the chemistry of iron oxide supported on γ–alumina and silica catalysts. ACS Omega 3:5362

42. Sokoll R, Hubert H, Schmuck I (1990) Thermal desorption and infrared studies of amines adsorbed on SiO_2, Al_2O_3, Fe_2O_3, MgO, and CaO. J Cat 125:276

43. Wang Z, Wang T, Wang Z, Jin Y (2006) The adsorption and reaction of a titanate coupling reagent on the surfaces of different nanoparticles in supercritical CO_2. J Colloid Interface Sci 304:152

44. Bayuo J, Bayetimani K, Bai P, Abukari M (2019) Adsorptive removal of hromium(VI) from aqueous solution unto groundnut shell. Appl Water Sci 9:107

45. Chen Z, Zhang S, Liu Y, Alharbi NS, Rabah SO, Wang S, Wang X (2020) Synthesis and fabrication of g-C3N4-based materials and their application in elimination of pollutants. Sci Total Environ 731:139054. https://doi.org/10.1016/j.scitotenv.2020.139054

46. Zhang S, Li B, Wang X, Zhao G, Hu B, Lu Z, Wen T, Chen J, Wang X (2020) Recent developments of two-dimensional graphene-based composites in visible-light photocatalysis for eliminating persistent organic pollutants from wastewater. Chem Eng J 390:124642. https://doi.org/10.1016/j.cej.2020.124642

47. Abd El-Latif MM, Ibrahim AM, El-Kady MF (2010) Adsorption equilibrium, kinetics and thermodynamics of methylene blue from aqueous solutions using biopolymer oak sawdust composite. J Am Sci 6:6

48. Schwantes D, Gonçalves A, Casarin CJ, Pinheiro A, Pinheiro IG, Coelho GF (2015) Removal of Cr(III) from contaminated water using industrial waste of the cassava as natural adsorbents. Afr J Agric Res 10:4241

49. Errais E, Duplay J, Darragi F, M'Rabet I, Aubert A, Huber F, Morvan G (2011) Efficient anionic dye adsorption on natural untreated clay: kinetic study and thermodynamic parameters. Desal 275(1):74–81

50. Tony MA, Lin LS (2020) Iron recovery form acid mine drain sludge as a Fenton source for municipal wastewater treatment. Int J Environ Anal Chem. https://doi.org/10.1080/03067319.2020.1734196

51. Kim D-H, Yang J-S, Baek K (2012) Adsorption characteristics of As(III) and As(V) on alum sludge from water purification facilities. Sep Sci Technol 47:2211–2217

52. Tony MA, Lin LS (2020) Attenuation of organics contamination in polymers processing effluent using iron-based sludge: process optimization and oxidation mechanism. Environ Technol. https://doi.org/10.1080/09593330.2020.1803417

53. Huang R, Yang B, Wang B, Zheng D, Zhang Z (2012) Removal of chromium (VI) ions from aqueous solutions by N-2-hydroxypropyl trimethyl ammonium chloride chitosan–bentonite. Desal Water Treat 50(1–3):329–337

54. Tony MA (2019) An industrial ecology approach: green cellulose based bio-adsorbent from sugar industry residue for treating textile industry wastewater effluent. Int J Environ Anal Chem. https://doi.org/10.1080/03067319.2019.1661397

55. Pan W, Zhang G, Zheng T, Wang P (2015) Degradation of p-nitrophenol using CuO/Al_2O_3 as a Fenton-like catalyst under microwave irradiation. RSC Adv 5:27043–27051